***In* Proceedings of Dragon Programme Mid-Term Results, Santorini, Greece 27 June-] July 2005 (ESA SP-611, January 2006). Pp 27-36**
2006
Ed H. Lacoste
ISBN 92-9092-922-7
https://archimer.ifremer.fr/doc/00706/81828/

Marine monitoring of the South- and East China Seas based on Envisat ASAR

Dagestad Knut-Frode [1], Johannessen Johnny [1], Kerbaol Vincent [2], Collard Fabrice [2], Kudryavtsev Vladimir [3, 4], Akimov Dmitry [4], Chapron Bertrand [5], Wang Hui-Jun [6], Wang Zifa [6], He Ming-Xia [7]

[1] Nansen Environm & Remote Sensing Ctr, Thormohlensgt 47, N-5006 Bergen, Norway.
[2] BOOST Technol, F-29280 Plouzane, France.
[3] Natl Acad Sci, Inst Marine Hydrophys, Sevastopol, Ukraine.
[4] Nansen Int Environm & Remote Sensing Ctr, St Petersburg, Russia.
[5] Inst Francais Rech Exploitat Mer, Plouzane, France.
[6] Chinese Acad Sci, Inst Atmospher Phys, Beijing, Peoples R China.
[7] Ocean Univ China, Ocean Remote Sensing Inst, Qingdao, Peoples R China.

Email addresses : knufd@nersc.no ; johnny.johannessen@nersc.no ; vincent.kerbaol@boost-technologies.com ; fabrice.collard@boost-technologies.com ; Vladimir.Kudryavtsev@niersc.spb.ru ; Dmitry.Akimov@niersc.spb.ru ; bertrand.chapron@ifremer.fr ; wanghj@mail.iap.ac.cn ; zifawang@mail.iap.ac.cn ; mxhe@orsi.ouc.edu.cn

Abstract :

Monitoring of the South- and East China Seas has been carried out for the period January to September 2005 with Envisat ASAR as the primary source of data. More than 130 Wide Swath scenes have been collected, showing a wide spectrum of oceanic features, such as current fronts, internal waves and wind generated surface waves, as well as rain cells, oil slicks, natural films and ships. Two software tools are here used to analyse the ASAR scenes: SARTool is a software developed for the analysis of SAR data for marine applications, and can be used to get quantitative estimates of wind and waves and to detect oil slicks and ships. The other tool used is the Radar Imaging Model (RIM), which couples a hydrodynamical model and a radar transfer model to calculate the radar backscatter that a SAR would measure for given wind speed and direction, surface current, surface film and, boundary layer stability, and radar geometry and wavelength. This paper shows some examples of applications of these two models to a selection of interesting ASAR scenes.

1 INTRODUCTION

Monitoring of the marine environment is important for many reasons: shipping and offshore industry need observations and forecasts of wind, currents and waves to improve safety and planning of operation; monitoring of oil spills can help the clean-up operation after major accidents and also quantify the amount of smaller spills from ships and oil-platforms for various regions, and mapping of offshore wind is of high interest as wind energy is the fastest growing source of renewable energy and since windmills are frequently placed offshore. In addition to such practical benefits, it is also important to observe the ocean to improve the understanding of the role of the ocean as a major component of the climate system. The Synthetic Aperture Radar (SAR) is a special type of microwave radar instrument which utilises the Doppler shift due to the movement of the satellite to get much finer resolution than would otherwise be possible: The "Advanced SAR" instrument (ASAR) onboard Envisat gives a pixel size of typically 10-150 metres, depending on mode of operation of the sensor and preprocessing of the signals. By comparison, pixel sizes are typically 1 kilometre for infrared and visible sensors onboard environmental satellites, and 5-50 kilometres for passive microwave instruments. Thus the (A)SAR gives the unique opportunity to get high resolution observations of several oceanic parameters, even at night and in the case of cloud cover. In this work, the Envisat ASAR is used to monitor the South- and East China Seas. This region is one of the busiest international sea lanes in the world, and more than half of the world's supertanker traffic passes through the waters of the region. In addition, the South China Sea region contains oil and gas resources strategically located near large energy-consuming countries. The fast economic growth of China and the other countries in the region is putting additional stress on the environment, and thus this area should be a natural focus area for marine monitoring.

2 STUDY AREA AND ACQUIRED ENVISAT ASAR DATA

The study area of this work are the South- and East China Seas (Fig. 1)

Proc. 2005 Dragon Symposium "Mid-Term Results", Santorini, Greece
27 June – 1 July 2005 (ESA SP-611, January 2006)

Fig. 1: Map of the South- and East China Seas. The red curve shows the typical path of the Kuroshio current.

A database system has been developed to automatically download, process and generate quicklooks of ASAR Wide Swath scenes for the area of interest from the Rolling Archive of ESA. This system permits spending more time on analysis of interesting scenes than on doing technical processing "by hand". For the period January to September 2005 more than 130 scenes have been downloaded and processed.

3 SOFTWARE TOOLS FOR ANALYSIS OF SAR DATA

ESA provides several free software tools for basic and general processing and plotting of Envisat satellite products (e.g. Beam, Best and Enviview). However, to derive secondary products for marine applications from SAR imagery, specialised tools are needed. Two such tools have emerged over the last years: SARTool and Radar Imaging Model ([1], [2], [3]). The following subsections describe briefly these two models, and Section 4 shows some examples of their applications.

3.1 SARTool

SARTool is developed by the French company "Boost Technologies" with the non-expert user in mind, and has an intuitive graphical user interface. It can read and process SAR images from the ERS, Radarsat and Envisat satellites. The program calibrates the scenes, and can do various image processing and geo-referencing for improved display. Additionally, it has modules to retrieve several scientific products: atmospheric wind speed and direction are calculated based on the influence on the ocean surface; wavelength, propagation direction and significant wave height can be calculated from Single Look Complex (SLC) images. It can detect ships and report the position, size, route and speed, and it can detect and report the position and size of oil spills. For more advanced users, SARTool can do multi-looks extraction from SLC images; estimate azimuth cut-off, and calculate moments and plot Pearson diagrams.

3.2 Radar Imaging Model

The mathematical model by Vladimir Kudryavtsev and others, described in [1], [2] and [3], combines a hydrodynamic module with a radar transfer module to calculate the radar signature (Normalised Radar Cross Section, NRCS) of the

sea surface if the following parameters are known: wind speed and direction; stability of the atmospheric boundary layer (parameterised with the air-sea temperature difference), ocean surface current, surface films and radar-parameters such as incidence and azimuth angles and radar wavelength. The model calculates the radar return (for both VV and HH polarisations) due to quasi-specular reflection, Bragg scattering and impact from breaking waves (foam/whitecaps), and also takes into account the feedback of breaking waves on shorter waves causing Bragg scattering. This model is developed into a computer code, here referred to as the "Radar Imaging Model" (RIM). Although this model is not easily inverted, it is useful to get a qualitative description of e.g. ocean currents, which are otherwise not easily detected from satellites, at least not in case of clouds.

4 EXAMPLES OF OBSERVED OCEANIC PHENOMENA

More than 130 ASAR WSM scenes from the South- and East China Seas have been collected and visually inspected, and many marine features have been identified. No systematic overview of all features will be given here, but rather some examples of features for which SAR-instruments are particularly useful. In the next subsections three ASAR-scenes are discussed: one showing the wind field related to a typhoon, one showing the signature of the Kuroshio current, and one showing the signature of internal waves.

4.1 The Typhoon "Khanun"

On 12 September 2005 the typhoon "Khanun" struck Shanghai and East China, and killed at least 14 people. This typhoon was observed with ASAR over the East China Sea the day before, 11 September at 01:47 UTC. The bright spiral seen on the ASAR Wide Swath Image in Fig.2 is not clouds, but increased radar backscatter due to wind generated roughness of the sea surface. With SARTool it is possible to apply the CMOD-algorithm to estimate the wind speed that generated the surface waves. One can choose between two versions of the algorithm; CMOD-IFREMER [4] which is the operational module for low to moderately high winds, and CMOD-5 [5] which is tailored to perform accurately for high wind speeds, and is expected to become operational. Fig.3 shows the wind speed of "Khanun" estimated with the CMOD5-algorithm. It is seen that ASAR reveals a high resolution variable wind field, with maxima of ~100 knots (~50 m/s). The direction of the wind speed is estimated from the ASAR scene by detecting wind streaks signatures in the FFT-transform of small subsets of the image.

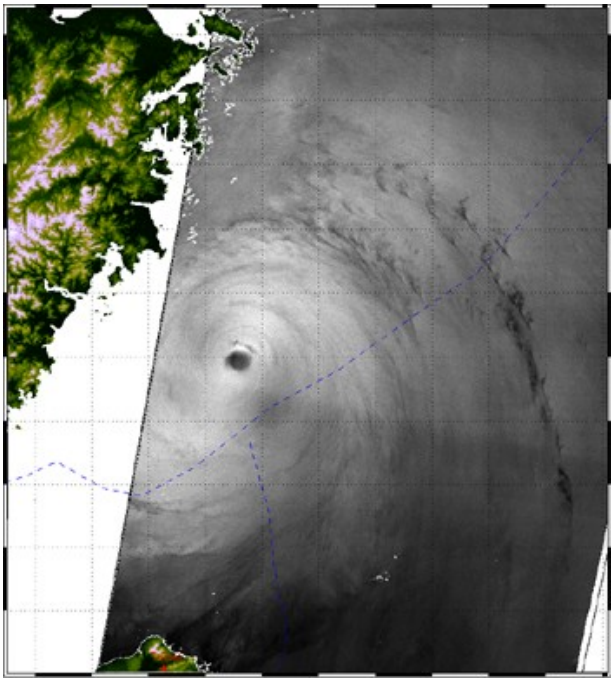

Fig. 2: Envisat ASAR Wide Swath image of the typhoon "Khanun" on 11 September 2005 01:47 UTC. The northern tip of Taiwan is seen at the bottom.

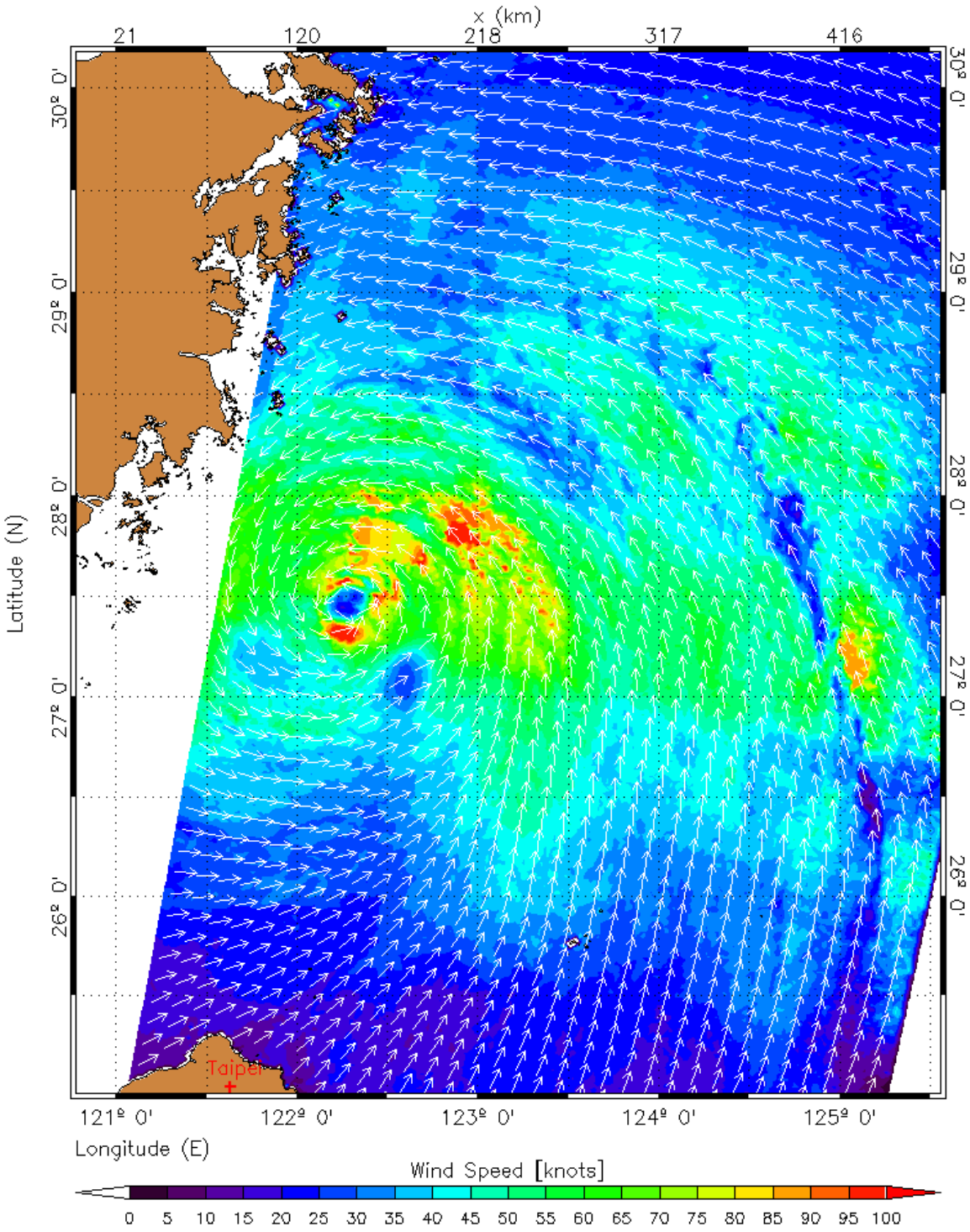

Fig.3: Wind speed for the typhoon "Khanun" calculated from the Envisat ASAR Wide Swath image in Fig. 2 using SARTool and the CMOD-5 algorithm. The arrows show the wind direction, calculated by detecting wind streaks signatures in the FFT-transform of small subsets of the image.

4.2 The Kuroshio current

Fig.4 shows an Envisat ASAR Wide Swath scene from the East China Sea on 13 July 2005 at 01:31 UTC. The location of the scene is indicated by the red box in Fig.5.

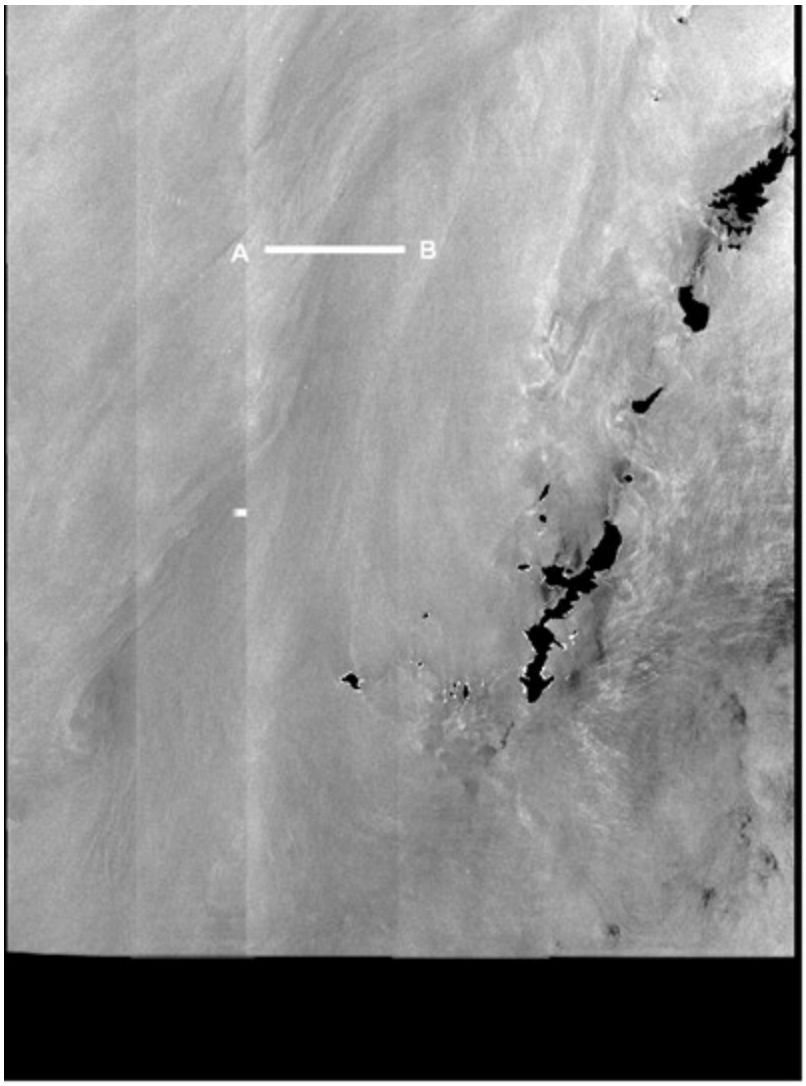

Fig. 4: Envisat ASAR WSM image over the East China Sea on 13 July 2005 at 01:31 UTC. The location of the scene is indicated with the red box on Fig. 5. The southernmost of the larger islands is Okinawa (Japan). Land is masked with black. The polarisation is VV, and the radar look direction is from the right (descending pass).

In the western part of the ASAR image one can see a structure stretching from the South-West to the North-East. Fig.5 shows the surface current field 1.5 hours prior to the ASAR acquisition for the East China Sea, assimilated into the Naval Coastal Ocean Model (NCOM) of the US Naval Research Laboratory. The structure on the ASAR image corresponds well with the strong surface current, exceeding 1 m/s, seen in the NCOM field. While there is little doubt that this is the Kuroshio current, the SAR imaging mechanism in this case is not evident. Fig. 4 shows that the current induces a decrease of the radar backscatter intensity, as seen e.g. over the transect from A to B. There are several mechanisms that can explain this feature.

One possibility is that convergence related to the current collects surface slicks, thus damping short surface waves and leading to a decrease of backscatter intensity. As the scene is from mid-summer (13 July), the primary production in the sea should be quite high, and surfactant films are probably abundant.

A second possible explanation is that the speed of the wind relative to the sea surface is lower across the current because the wind and current have the same direction. This explanation is supported by Fig.6, which shows that the wind direction derived from QuikSCAT is mainly along the Kuroshio current in this region the actual day. This figure also shows the speed of the wind, estimated by SARTool using the CMOD-IFREMER algorithm. The wind speed in the region around Kuroshio is about 8 m/s. Thus, since the model field of Fig.5 shows a maximum current speed of more than 1 m/s, the wind speed relative to the sea surface is about 13 percent lower than for the surrounding region where the speed of the current (according to the assimilated model field) is much smaller, and where the current is less directed along the main pathway of the Kuroshio current (Fig. 5).

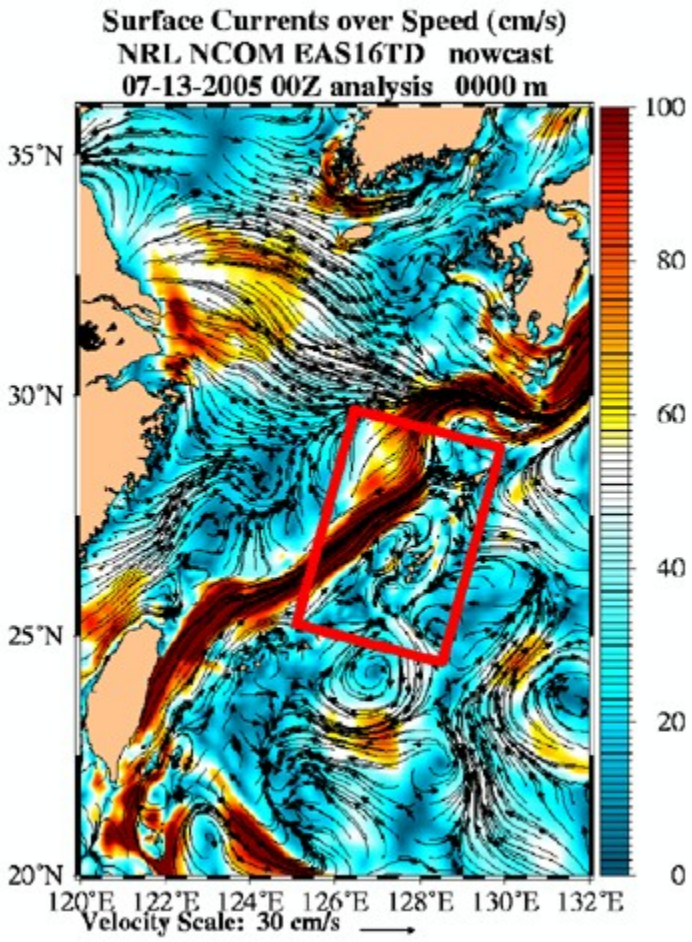

Fig. 5: The assimilated surface current field for the Naval Coastal Ocean Model of the US Naval Research Laboratory. The time corresponds to 1.5 hours prior to the acquisition of the Envisat ASAR scene of Fig.4 (position indicated by the red box).

A third explanation is due to hydrodynamic modulation of the ocean surface waves, caused by complex interaction between the current and waves at different scales, and further affected by breaking waves. Such complex interaction can be difficult to explain (and intuitively understand), but the Radar Imaging Model (Section 3.2) can assist the interpretation. For example, the model can be used to calculate the radar signature corresponding to divergent, convergent, or shear currents, which can then be compared to the SAR image. Here the model will be used to simulate the NRCS corresponding to the transect A-B of Fig.4. Similarly to [6], a hyperbolic tangent function will here be used to simulate such currents to be input to the RIM model:

$$F(x) = \frac{(1 + tanh(x/L))}{2} \tag{1}$$

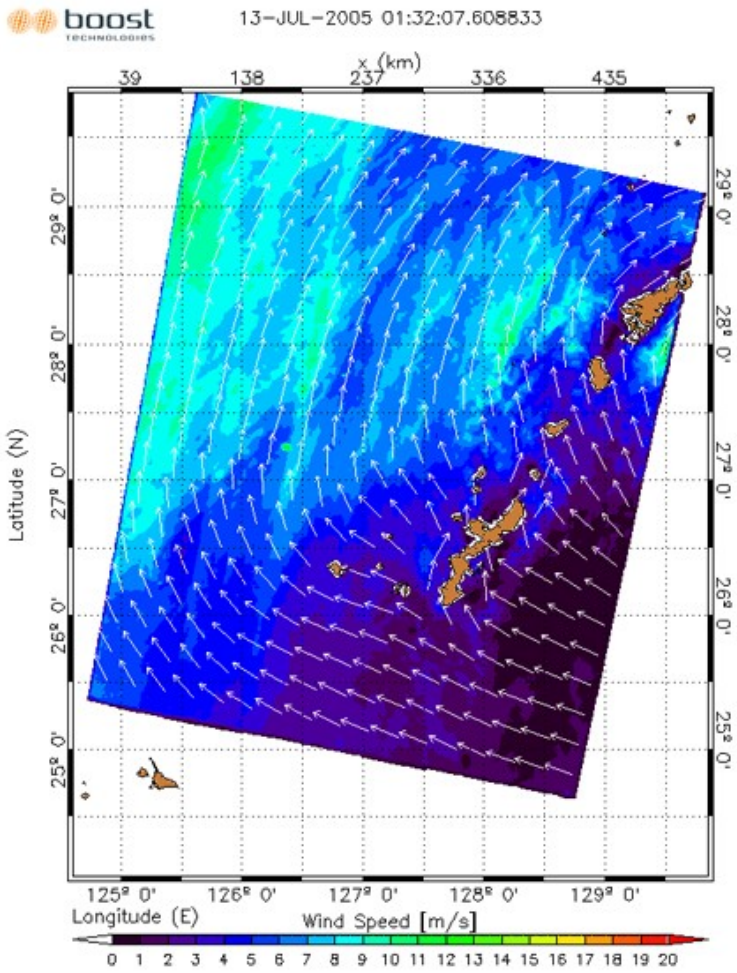

Fig. 6.: High resolution wind speed field (colours) for the ASAR image of Fig.4. This is estimated with SARTool using the CMOD-IFREMER algorithm. Also input to the algorithm is the wind direction field from QuikSCAT (white arrows). The QuikSCAT wind direction field is from a daily gridded dataset (12-13 July 2005), freely available from ftp://ftp.ifremer.fr/ifremer/cersat/products/gridded/mwf-quikscat/data/daily/

Here x is the distance perpendicular to the current, e.g. increasing from A to B in Fig.4, and the scale parameter L is taken as 250 metres. The three different current types are defined by:

$$\begin{aligned} U = F(x),\ V = 0 &\quad \text{for a divergent current} \\ U = -F(x),\ V = 0 &\quad \text{for a convergent current} \\ U = 0,\ V = F(x) &\quad \text{for a shear current} \end{aligned} \tag{2}$$

Other parameters input to RIM can be estimated from Figs. 4 and 6: Corresponding to the cross section A-B indicated on Fig.4, the incidence angle is taken as 35 degrees, and the radar look angle is in the negative x-direction. A constant wind speed of 8 m/s is used, in the direction of the V-component of the current (perpendicular to the x-axis and radar look direction). The simulated Normalised Radar Cross Section (NRCS) for the three different current properties is plotted in Fig.7. For the divergent current there is a decrease of the NRCS in the convergence zone, qualitatively similar to what is seen in the ASAR scene in Fig.4. The shear current creates contrast on the same order of magnitude as the divergent current, but there is not an overall decrease of the NRCS in the shear zone, and thus the shear current does not

explain the dark band seen on Fig. 4. A convergent current, however, induces a brightness peak, thus opposite of what is observed.

Different stability of the atmospheric boundary layer can also cause signatures on the ocean surface because of variations in the transfer of momentum across the air-sea boundary. Variations in the sea surface temperature (SST), often the case over current zones, can cause such variations of the atmospheric stability. For this particular case, however, the assimilated (from AVHRR) SST for the NCOM model showed (not shown here) rather uniform temperatures across the Kuroshio current.

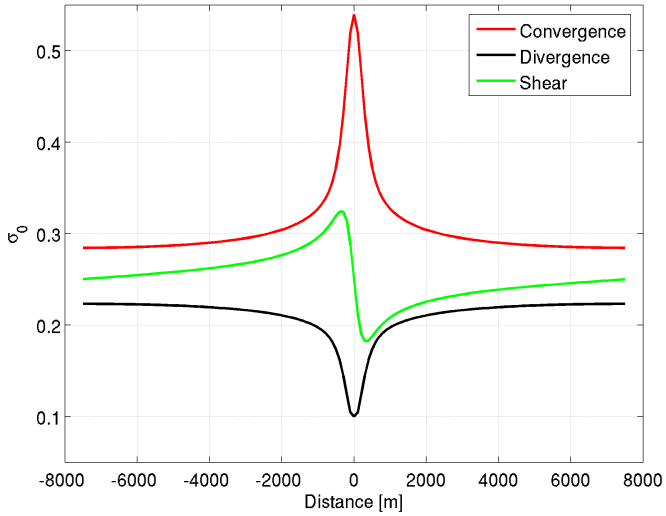

Fig. 7: Normalised Radar Cross Section (σ_0) (C-band, VV polarisation) simulated with the RIM model (Section 3.2) for convergent, divergent and shear currents defined by Eqs. 1 and 2. The radar look direction is perpendicular to the current fronts (from the right); the incidence angle is 35 degrees and the wind speed is 8 m/s along the front (positive y-direction).

4.3 Internal waves

Fig.8 shows an Envisat ASAR WSM scene from the South China Sea, around the Dongsha Islands (Fig. 1), acquired 27 March 2005. This is a typical scene from the South China Sea, where there is an abundance of expressions of internal waves. The internal waves are generated in the Luzon Strait (between Taiwan and the Philippines (Luzon Island)) by the tidal wave as it propagates westwards and interacts with the bathymetry (Werner Alpers, personal communication). The distance between the waves 'A' and 'B' in Fig.8 is measured with SARTool to be 75 kilometres. Thus, if they are generated from the semi-diurnal tidal component, the distance travelled corresponds to a speed of 1.7 metres per second, which is reasonable. If the depth of the mixed layer is small compared to the total depth and the wavelength, the speed of the internal waves can be approximated by:

$$c = \sqrt{(gH \frac{\delta \rho}{\rho})} \tag{3}$$

where g is the gravity acceleration, and $\delta\rho/\rho$ is the relative difference in density between the mixed layer and the lower layer. Taking $\delta\rho/\rho$ to be 0.002, Eq. 3 gives a mixed layer depth H of 147 metres.

The Radar Imaging Model nicely reproduces the increased radar brightness caused by such internal waves, see e.g. Fig.13 of [3]

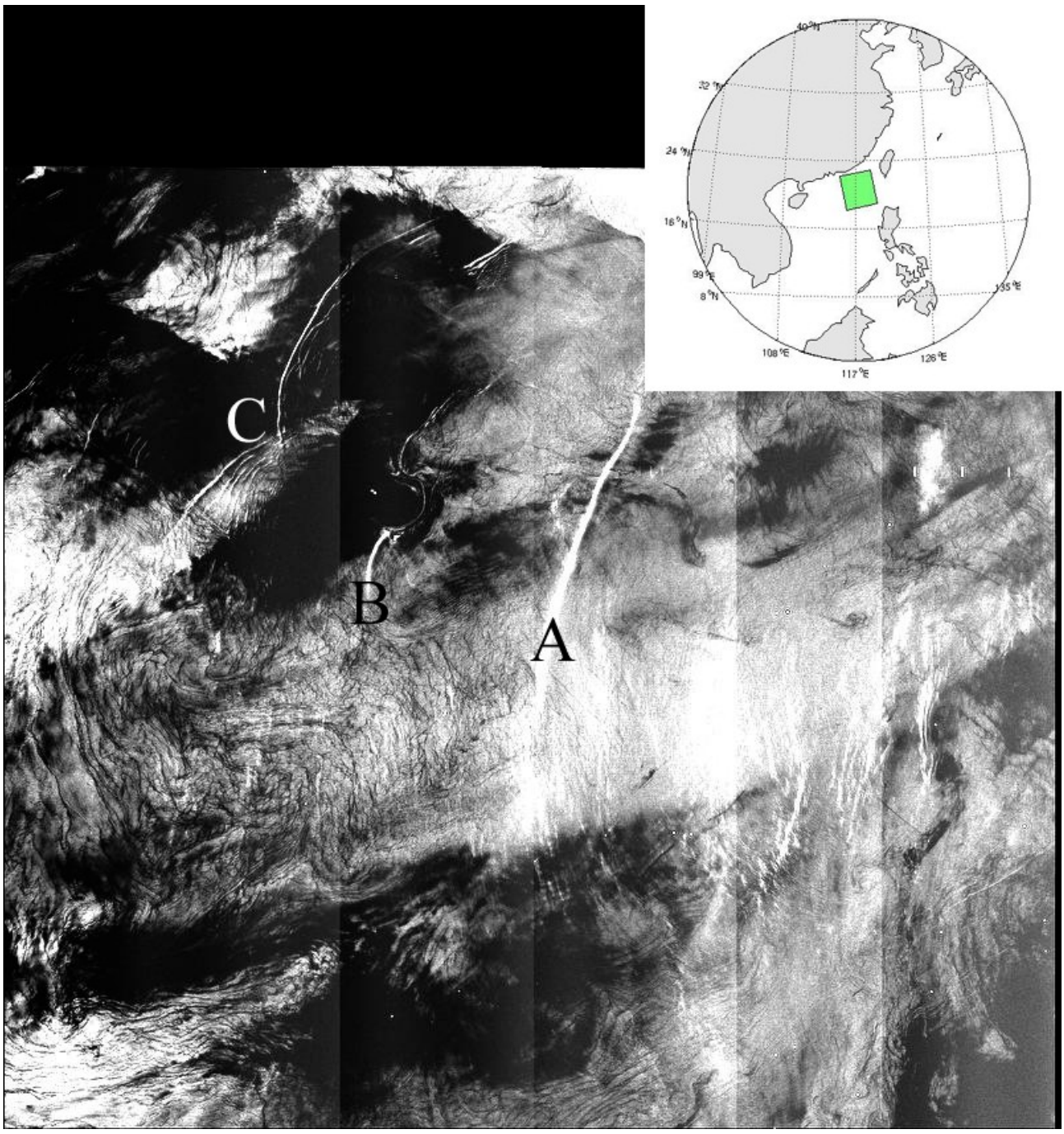

Fig.8: An Envisat ASAR WSM scene from the South China Sea acquired on 27 March 2005 at 14:13 UTC. The letter 'A' marks the signature of an internal wave travelling to the west. 'B' shows an internal wave interacting with and being diffracted at the Dongsha (Pratas) Islands. 'C' shows a diffraction pattern of internal waves refracted at an earlier time. The distance from 'A' to 'B' is 75 kilometres.

5 CONCLUSIONS AND FUTURE PROSPECTS

More than 130 ASAR Wide Swath scenes over the East- and South China Seas have been collected for marine monitoring. Here three interesting scenes are discussed:

The first image shows the typhoon “Khanun” which struck China on 12 September 2005. Using the software SARTool and the CMOD-5 algorithm [5], a high resolution wind field with maxima exceeding 50 m/s is found around the eye of

the typhoon.

The second image shows a band of lower radar backscatter which corresponds well in time and space with a region of strong (> 1m/s) ocean surface current from the Naval Coastal Ocean Model (NCOM) of the US Naval Research Laboratory. Using the Radar Imaging Model ([1], [2] and [3]), hydrodynamic modulation of ocean waves due to divergent current is suggested as a reason for the signature on the ASAR scene, rather than convergent or shear currents. Other possible (additional) mechanisms suggested are collection of surfactant slicks due to convergent currents (thus an opposite effect of the hydrodynamic modulation due to divergent currents) or less impact of the wind on the sea surface due to coincident current and wind direction.

The third ASAR scene shows a train of internal waves travelling westwards in the South China Sea, and being refracted at the Dongsha Islands. The propagation speed of the waves is estimated to 1.7 m/s and the depth of the mixed layer is estimated to be 147 metres.

Synergy with other satellite sensors, model data or *in situ* data is seen to be very useful in assisting the interpretation of ASAR images. In the near future efforts will be spent on creating an efficient system for collecting and collocating imagery from other sensors (e.g. MERIS and AATSR) with ASAR scenes. In this work, an ASAR scene has been qualitatively compared with output of the NCOM ocean model. In the future more quantitative comparisons will be made, by e.g. calculating the surface velocity deformation field which is more suitable for comparison with SAR features [6].

The software tools used here are quickly evolving, and an idea is launched to include the Radar Imaging Model into the more easy-to-use SARTool. This idea will also consider to adopt the new algorithm developed to measure ocean surface velocity directly from space from the Doppler signal recorded by ASAR [7].

REFERENCES

1. Kudryavtsev, V., D. Hauser, G. Caudal, and B. Chapron, A semi-empirical model of the normalized radar cross-section of the sea surface. Part 1: The background model, J. Geophys. Res., 108, C3, doi:10.1029/2001JC001003, 2003.
2. Kudryavtsev, V., D. Hauser, G. Caudal, and B. Chapron, A semi-empirical model of the normalized radar cross-section of the sea surface. Part 2: Radar modulation transfer function, J. Geophys. Res., 108, C3, doi:10.1029/2001JC001004, 2003.
3. Kudryavtsev V., D.Akimov, J.A.Johannessen, and B. Chapron, On radar imaging of current features. Part 1: Model and comparison with observations, J.Geoph.Res., 110, C07016, doi:10.1029/2004JC002505, 2005.
4. Quilfen, Y., Chapron, B., Elfouhaily, T., Katsaros, K., Tournadre, J., and Chapron, B., Observation of Tropical Cyclones by High-Resolution Scatterometry, J. Geophys. Res., 103, 7767-7786, 1998.
5. Hersbach H, CMOD5 an improved geophysicalmodel function for ERS C-band scatterometry, Internal report, European Centre for Medium-Range Weather Forecast, 2003.
6. Johannessen, J. A., V. Kudryavtsev, D. Akimov, T. Eldevik, N. Winther, and B. Chapron, On radar imaging of current features. Part 2: Mesoscale eddy and current front detection, J.Geoph.Res., 110, C07017, doi:10.1029/2004JC002802, 2005.
7. Chapron, B., F. Collard, and F. Ardhuin, Direct measurements of ocean surface velocity from space: Interpretation and validation, J. Geophys. Res., 110, doi:10.1029/2004JC002809, 2005.

- *SARTool web page: http://www.boost-technologies.com/web/en/sartool.html*
- *NCOM EAS16 model web page: http://www7320.nrlssc.navy.mil/EAS16_NFS/TIDES/EAS16NFS.html*